APCC
APEC CLIMATE CENTER

TECHNICAL REPORT

APCC
APEC CLIMATE CENTER

PREFACE

It is our pleasure to present to you the APEC Climate Center (APCC)'s Technical Report 2012, which reports the core outcomes of our research activities from the past year.

Since 2005, APCC, as a hub of climate information in the Asia-Pacific region, has strived to share our analysis and prediction of abnormal climate and to apply this information to regional development. The Center has established the most extensive Multi-Model Ensemble (MME) system for seasonal prediction in the world through its international science network and has provided value-added products to various stakeholders. Recently, APCC has expanded its mandate to include enhancing the capacity of APEC member economies to respond effectively to climate change and variability through better application of climate information.

In 2012, APCC continued to make an effort to improve the quality and quantity of our short-term climate forecasts and our online climate information systems, as information dissemination tools. Additionally, APCC began its endeavor to produce more applicable climate information through interdisciplinary research among various sectors, such as agriculture and hydrology. The following technical report provides more information about our research outcomes from 2012.

In 2013, following APCC's goal to enhance socioeconomic well-being through better utilization of climate information, APCC will continue to improve the quality and accuracy of its climate information, recognizing that the utility of this information is only as good as its quality. We would like to make the best use of our research outcomes in various scientific and application areas. We welcome any feedback on this report or on our services.

My best and warmest regards to all of you.

Dr. Chin-Seung Chung
Director/APEC Climate Center

CONTENTS

The Role of the West Pacific Teleconnection Pattern in Changing the Seasonal Footprinting Mechanism over the Pacific Ocean

■■ Mr. Ji-Won Kim

APCC

TECHNICAL REPORT 2012-03

The Role of the West Pacific Teleconnection Pattern in Changing the Seasonal Footprinting Mechanism over the Pacific Ocean

Mr. Ji-Won Kim

ABSTRACT

The western Pacific oscillation (WPO) teleconnection pattern, which consists of a north-south meridional dipole structure with one center located over the Kamchatka Peninsula and another broad center of opposite sign covering portions of southeastern Asian and the western subtropical North Pacific, is one of the primary modes for low-frequency variability in conjunction with the North Pacific Oscillation (NPO) variability over the North Pacific. In this study, the specific role of the WPO teleconnection pattern in changing the connection between the mid-latitude and tropical Pacific variability, as known as "Seasonal Footprinting Mechanism (SFM)", is investigated. Analogous to the NPO variability, the boreal wintertime WPO atmospheric forcing is also able to generate the SFM process with stronger North Pacific Gyre Oscillation (NPGO) climate pattern. Two conditional cases regarding the NPO and WPO are composed in order to identify the specific role of the WP variability: when the NPO only occurs without WPO (i.e., NPO_only), and when the NPO coincides with WPO (i.e., NPO+WPO). Using a conditional composite analysis, it is found that the NPO and WPO atmospheric structures are not the same that the location of the WPO variability is significantly shifted westward compared to that of the NPO variability over the North Pacific. Furthermore, our analysis suggests that when the NPO and WPO simultaneously occur during the winter, a stronger NPGO mode is activated via changes in the surface net heat flux anomalies and equatorward moving anomalous warm temperature and westerly wind stress presumably caused by the weakened polar jet stream. These changes eventually result in the central Pacific-type El Niño structure as opposed the eastern Pacific-type El Niño structure generally induced by the NPO_only-related atmospheric forcing. Long-term coupled general circulation model analysis further verifies the observational results, showing a center-concentrated warming structure over the equatorial Pacific region in the following winter when the NPO coincides with the WPO in the previous winter.

1. INTRODUCTION

Understanding connections between tropics and mid-latitudes over the ocean-atmosphere system has been consistently stressed in illuminating the mechanism as well as the potential predictability of its associated impacts on the weather and climate variability in the mid-latitudes (Arkin 1982; Pan and Oort 1983; Hoerling *et al*. 1997; Newman and Sardeshmukh 1998; Mo and Higgins 1998; Barnett *et al*. 1999; Alexander *et al*. 2002; Straus and Shukla 2002; An and Wang 2005; Yeh and Kirtman 2008). The El Niño-Southern Oscillation (ENSO) is able to affect the extratropical climate via the so-called "atmospheric bridge" teleconnection on an

interannual time scale (Alexander 1992; Lau and Nath 1996). In details, ENSO can alter the spatial structure of heating over the tropics and provides a vorticity source for poleward propagating Rossby waves, which then influence the atmospheric circulation through an interaction with the mean state in the mid-latitudes.

It has also been convincingly argued that atmospheric forcing initiated in the North Pacific may contribute to changes of SST variability on interannual to decadal timescales though, the westerly wind bursts in the central-western tropical Pacific (Yu and Rienecker 1998; Nakamura *et al*. 2006, 2007), advection to the equator of fluctuations in the temperature and salinity created by air-sea interaction in mid-latitudes (Gu and Philander 1997), and altering the volume of cold water reaching the equator induced by the changes in extratropical winds (Kleeman *et al*. 1999; McPhaden and Zhang 2002).

In addition, recent studies have emphasized that the North Pacific Oscillation (NPO; Walker and Bliss 1932; Rogers 1981), an intrinsic wintertime atmospheric variability in the second leading pattern of the atmospheric circulation over the North Pacific, plays a prominent role in affecting tropical variability through the so-called "Seasonal Footprinting Mechanism (SFM)" (Vimont *et al*. 2003a, b) and other subsequent studies. The overall physical processes of the SFM are explained as follows: because the intrinsic mid-latitude atmospheric variability is most energetic in the winter months, the NPO-forced SST anomalies in the North Pacific maximize during the boreal late winter and early spring. The SST anomaly pattern driven by the NPO forcing, via changes in the surface net heat flux, is called an "SST footprint", or the North Pacific Gyre Oscillation (NPGO; Di Lorenzo *et al*. 2008) climate pattern, which is considered to be the oceanic expression of the forcing of the NPO (Ceballos *et al*. 2009). This SST footprint (or NPGO pattern) persists into the following summer, when the mid-latitude atmosphere is more quiescent. During summer, the SST footprint diminishes and an atmospheric circulation anomaly in the subtropics forces zonal wind stress anomalies that excite the oceanic equatorial Kelvin wave signals. These excited Kelvin waves propagate eastward, depressing the thermocline in the central and eastern tropical Pacific, which in turn increases the SST anomalies in these areas through the eastward advection of warm water and the reduction of upwelling. These

anomalies continue to grow during the next winter, resulting in an El Niño-like structure in the eastern tropical Pacific. The SFM is now being deemed as a possible mechanism to lead the El Niño-like warming from the mid-latitudes.

Meanwhile, there is another predominant mode of mid-latitude wintertime atmospheric variability; the Western Pacific Oscillation (WPO; Wallace and Gutlzer 1981), which shows a meridional dipole structure and which is slightly shifted to the western Pacific in comparison with the NPO structure. The WPO is characterized by a center over the Kamchatka Peninsula with a broad low-latitude node straddling the 155°E meridian and a cold-core equivalent barotropic structure. The NPO, however, consists of a meridional dipole in sea level pressure (SLP) over the central Pacific roughly located at 170°W with centers at approximately 35° and 60°N. It is known that strong positive and negative phases of the WPO reflect pronounced zonal and meridional variations in the location and intensity of the entrance regions of East Asian jet stream (Wallace and Gutlzer 1981; Barnston and Livezey 1987), on the other hand, the NPO is more associated with the variations of Aleutian low over the northeastern Pacific.

Here is a lack of full documentation on the physical mechanisms and hemispheric climate impacts of the WPO, owing to the limited focus of research in comparison with that focused on the NPO. One of the main reasons for such little attention is that the WPO was thought to have a similar variability to that of the NPO (e.g., Linkin and Nigam 2008). As the relationship between the WPO and the relevant related SFM process has not been well-investigated due to such emphasis in spite of the fact that the WPO and NPO have different atmospheric structures, it is considered particularly important to direct focus towards this. The purpose of this study is therefore to identify the specific role of the WPO in changing the SFM process over the Pacific Ocean in comparison with the NPO. According to the recent studies, it has been argued that the NPO-like atmospheric dipole pattern and its derived NPGO mode are intimately tied to variability in central equatorial Pacific SSTs associated with the El Niño-Modoki/Central Pacific warming at low-frequencies (Ashok *et al*. 2007; Weng *et al*. 2007; Di Lorenzo *et al*. 2010; Furtado *et al*. 2012). Furthermore, Park *et al*. (2012) reported that the ENSO variability triggered by the SFM process

has a favorable NPO structure during the previous winter via two different conditional cases, NPO-El Niño and NPO-normal. It is implying that subtle differences of the wintertime NPO-like spatial structures over the North Pacific are sensitive to determining the changes in the tropical Pacific SST variability during the following seasons. Thus, it is important to understand how the WPO has influence on the connection between atmospheric structures over the North Pacific and tropical Pacific SSTs in conjunction with the NPO.

This study is organized as follows: Section 2 provides a brief description of the data sets and methodology utilized in this study. Section 3 illustrates the general features of the SFM process driven by the positive NPO and WPO forcings. In Section 4, the role of the WPO in changing the SFM process in connection with the NPO is described, by means of a conditional composite analysis and plausible interpretations are also served in Sect. 4.2. Furthermore, the findings in this study are verified using the long-term climate simulation of the coupled general circulation model (CGCM), which is adopted in the phase 5 of the Coupled Model Intercomparison Project (CMIP5). Finally, the main results are summarized and discussed in section 5.

2. Data and methodology

2.1 Reanalysis data

The atmospheric variables utilized in this study are SLP, geopotential height (GPH), air temperature, the zonal and meridional surface wind and momentum flux, and surface net heat flux calculated by aggregating shortwave and longwave radiation and sensible and latent heats, respectively. The data are obtained from the National Centers for Environmental Prediction-National Center for Atmospheric Research (NCEP-NCAR) reanalysis 1 (available online at ftp://ftp.cdc.noaa.gov/Datasets /ncep.reanalysis.derived/). Details regarding this dataset, including the physics and dynamics of construction and its numerical and computational methods, are described in Kalnay *et al.* (1996) and Kistler *et al.* (2001). The variable SLP has a 2.5° (latitude)

× 2.5° (longitude) spatial resolution, while other variables have uneven spatial resolutions on 192 × 94 Gaussian grids. The SST data is the National Oceanic and Atmospheric Administration (NOAA) Extended Reconstructed SST version 3b (ERSSTv3b) on a 2.0° × 2.0° grid, which is the most recent version of the ERSST analysis (Smith *et al*. 2008; http://www.esrl.noaa.gov/psd/data/gridded/). The analysis period of the datasets spans from January 1958 to December 2011; chosen because of the increased observations after the International Geophysical Year.

2.2 Coupled general circulation model

The Geophysical Fluid Dynamics Laboratory (GFDL) Climate Model version 3 (CM3) CGCM is employed to verify the observational results. The GFDL-CM3 model is an update of the GFDL-CM2.1 model (Delworth *et al*. 2006), and is adopted in the CMIP5, which includes generally higher resolution models and a broader set of experiments relative to CMIP3 (Taylor *et al*. 2012). The output of GFDL-CM3 model is now applied to simulate climate change for the Intergovernmental Panel on Climate Change Fifth Assessment Report (IPCC AR5). The major developmental effort for CM3 is focused on the atmosphere component, which is an update from the CM2.1 atmospheric component (AM2; GFDL GAMDT, 2004) to the new AM3 component in CM3 (Donner *et al*. 2011). In addition, the CM2.1 land component, LM2, was exchanged for a new land component, LM3 (Milly *et al*. in prep). The LM3 improves on LM2's physical representations of the flow of heat and water through the land. A dynamical vegetation component was added to the land model and direct and indirect aerosol effects were also included. The CM2.1 sea ice (SIS) and ocean (MOM) components remain essentially unchanged in CM3 (Griffies *et al*. 2011). In this study, we analyze a 500-yr preindustrial control run simulation (i.e., piControl in CMIP5 experiment description), which was performed following the CMIP5 protocol (Taylor *et al*. 2012), with fixed values for atmospheric composition, land cover, and insolation based on data for the year 1860. The initial conditions from this experiment were taken from January 281 of the 1860 control model spin-up experiment. The data are now available in the CMIP5 archives (available online at http://pcmdi9.llnl.gov/esgf-web-fe/).

2.3 Climatic index and methodology

We applied the conditional composite analysis as a primary methodology by using the NPO and WPO indices. The NPO index, as shown in Fig. 1(a), was defined using the second Empirical Orthogonal Functions (EOF) principle components (PC) time series of boreal winter SLP anomalies in the North Pacific (20–70°N, 110°E–90°W) (i.e., during November-December-January-February-March, with the 5-month period hereafter denoted by the first letter of each respective month, NDJFM). The WPO index for the winter (NDJFM) provided by the NOAA Climate Prediction Center (NOAA CPC; available online at ftp://ftp.cpc.ncep.noaa.gov/wd52dg/data/indices/wp_index.tim) is also represented in Fig. 1(b). The WPO index is based on centers-of-action of 500-hPa height patterns and computed by subtracting area-averaged value over 50–70°N, 140°E –150°W from 25–40°N, 140°E–150°W. In the present study, the WPO index is inverted multiplying by -1 to alter the signs into the same phase as the NPO index. The boreal wintertime SLP-regressed patterns with respect to the NPO and WPO indices exhibit a similar north-south meridional dipole spatial structure over the North Pacific (not shown). We refer to this dipole structure as a positive phase of the NPO and WPO, which briefly includes an anomalous high pressure over the Bering Sea and anomalous low pressure near Hawaii. Anomalies used in this study are presented as values after removing the monthly-mean climatological seasonal cycle and linear trends for the whole period. The statistical significances of temporal and spatial correlation coefficients and composite differences are assessed using a two-tailed Student's *t*-test (Wilks 2006) unless otherwise stated.

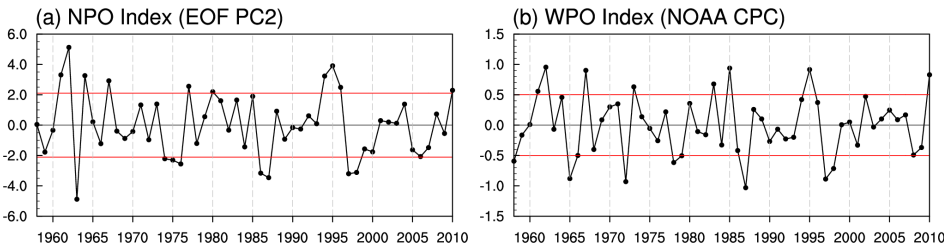

Figure 1 (a) The NPO index calculated by the EOF second principal components (PC2) of boreal winter (NDJFM) sea level pressure (SLP, in hPa) anomalies in the North Pacific (20-70°N, 110°E-90°W). (b) is the same as (a) but uses the WPO index obtained from NOAA CPC. Red horizontal lines represent ±1 standard deviation. A detailed description of each index is given in Section 2.3.

3. NPO-/ WPO-induced Seasonal footprinting mechanism

According to the SFM process, NPO-like intrinsic mid-latitude atmospheric variability during the previous winter can affect the tropical ENSO variability during the following winter. In order to identify whether the positive NPO and WPO forcings could be effective in inducing the El Niño structure, a composite analysis was conducted using the NPO and WPO years. For preprocessing, NPO and WPO years are firstly defined as years during which each of the two indices is more than one standard deviation above the mean (see Fig. 1). As seen in table 1, nine years of NPO and seven years of WPO were chosen as positive forcings during the study period. Because the NPO and WPO variability have a close relationship, the years of 1961, 1962, 1967, and 1995 are periods when the NPO and WPO occur simultaneously (cf. temporal correlation coefficient between the two indices is 0.65, exceeding 99% confidence level).

Figures 2(a)–(c) show the composite maps for the NPO years of the SLP anomalies during ND(-1)JFM(0), the SST and horizontal wind stress (UVFLUX) anomalies during April-May-June-July-August (AMJJA(0)), and the SST anomalies during October-November-December-January-February (OND(0)JF(+1)). Note that the wind stress anomalies (red arrows) are only expressed when they are statistically significant at the 90% confidence level. As expected, it is confirmed that the positive NPO forcing during the previous winter (Fig. 2(a)) precedes the El Niño the following winter (Fig. 2(c)) via the summer SST footprint onto the ocean invoked by the NPGO pattern with westerly wind stress anomalies in the central tropical Pacific (Fig. 2(b)). This result is almost consistent with that of previous studies (Vimont *et al*. 2003a, b; Alexander *et al*. 2010; Park *et al*. 2012). In addition, the Pacific Meridional Mode (MM, Chiang and Vimont 2004; Chang *et al*. 2007) is also found in Fig. 2(b), which manifests the SST anomalies of one sign extending southwestward from Baja California to the central-western equatorial Pacific with anomalies of the opposite sign in the eastern equatorial Pacific. The MM is a thermodynamical coupled mode driven by the wind-evaporation-SST (WES) feedback (Xie and Philander 1994), which includes variations in the meridional SST gradient and the intertropical convergence zone (ITCZ) and which eventually affects the evolution of the ENSO variability through the SFM process.

Likewise, figures 2(d)–(f) show the same composite maps for the WPO years. The winter SLP anomaly pattern caused by the positive WPO forcing (Fig. 2(d)) is almost similar to that of the NPO forcing (cf. pattern correlation coefficient between Fig. 2(a) and 2(d) is 0.93). Given the WPO characteristics, it is found that the southern lobe of the WPO dipole pattern is slightly enhanced and expanded to the western Pacific when compared to that of the NPO dipole pattern. The subsequent SST anomaly structure during the following summer clearly corresponds to the NPGO pattern with strong magnitudes, and the equatorial westerly wind stress anomalies are significantly increased, mainly located in the northwestern tropical Pacific (Fig. 2(e)). By the way, the following winter SST anomaly structure (Fig. 2(f)), which is induced by the WPO forcing, is quite different from the NPO-induced El Niño structure (see Fig. 2(c)), imposing a central Pacific warming although the signals are quite weak and insignificant. It implies that the WPO forcing could be another feasible candidate to generate the SFM process and play a role in modulating the ENSO variability during the next winter differently from the NPO forcing.

Table 1 NPO and WPO years defined as years during which each of two indices is more than one standard deviation above the mean. Year 1961, for example, refers to the boreal winter of 1961/1962.

	Year
NPO (9)	1961, 1962, 1964, 1967, 1977, 1980, 1994, 1995, 1996
WPO (7)	1961, 1962, 1967, 1973, 1983, 1985, 1995

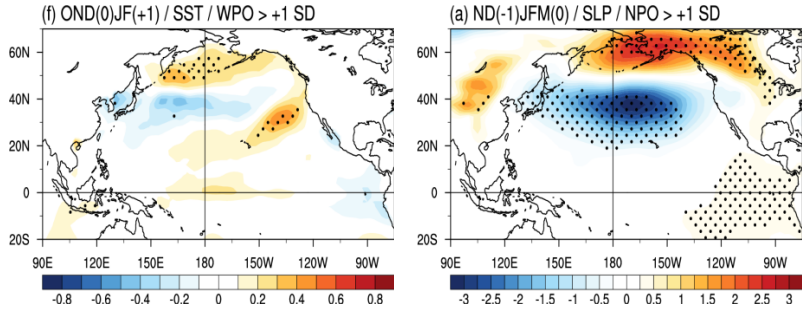

Figure 2 Composites of the anomalous (a) sea level pressure (SLP, in hPa) during the previous winter (ND(-1)JFM(0)), (b) sea surface temperature (SST, in oC) and horizontal momentum flux (UVFLUX, in N/m2) during the following summer (AMJJA(0)), and (c) SST during the following winter (OND(0)JF(+1)) for the NPO years. (d), (e), and (f) are the same as (a), (b), and (c), except they represent the WPO years. Areas with black dots and red arrows indicate a 90% confidence level according to a two-tailed Student's *t*-test.

4. Results

4.1 Comparison between NPO_only and NPO+WPO

In order to clarify the specific role of the WPO in changing the SFM, compared to the sole effect of the NPO, we composed two conditional cases termed the NPO_only and NPO+WPO. The NPO_only is defined as the years when the NPO occurs in exclusion of the WPO years and the NPO+WPO is defined as the years when the NPO coincides with WPO years. According to the definitions, the NPO_only occurs in five years (1964, 1977, 1980, 1994, and 1996) and the NPO+WPO case occurs in four years (1961, 1962, 1967, and 1995) (cf. Table 1). The wintertime SLP and GPH anomalies at 700- and 300- hPa levels for both the NPO_only and NPO+WPO composites are shown in Fig. 3. In the NPO_only, the full hemispheric view shows a distinctive positive NPO forcing with a north-south dipole structure over the North Pacific basin, with its centered located over 170°W longitude and 40°N (southern lobe) and 60°N (northern lobe) latitude (Fig. 3(a)). This is a typical NPO signature with its characteristic dipole pattern. The upper-air GPH structures at 700- and 300-hPa levels have a strong resemblance to the SLP structure because of the pronounced equivalent barotropic structure (Fig. 3(b) and 3(c)). These vertical atmospheric characteristics of the NPO_only forcing have been well-documented in previous literature (Wallce and Gutlzer 1981; Horel 1981; Hsu and Wallace 1985; Barnston and Livezey 1987; Nigam 2003).

Differences are noted in the vertical atmospheric structures of the NPO+WPO and the NPO_only. In the high-latitudes, anomalous high pressure circulations (i.e., anticyclonic circulation) are clearly observed with a triple centered positioned near Siberia, the eastern Aleutian Islands and the Far North Atlantic, broadly possessing the Arctic polar region although there is an anomalous low pressure circulation (i.e., cyclonic circulation) over the Kara Sea and the Laptev Sea (Fig. 3(d)). These patterns are spatially coherent with increasing height (Figs. 3(e)–(f)) and hence a weakened upper-air circulation arises, which is reminiscent of a weakening of the polar-front jet stream that exists on the boundary between polar and mid-latitude air. The dipole GPH anomaly pattern over the North Atlantic is likely to be indicative of the negative

North Atlantic Oscillation (NAO; Rogers 1984). In addition, southern lobe of the NPO+WPO over the North Pacific is more zonally elongated and shifted westward compared with that of the NPO_only (Fig. 3(d)). As height increases, the low pressure structure in the southern lobe of the NPO+WPO is separated into two cores that one is broadly located at 170°W and the other is at 135°E (Figs. 3(e)–(f)). By definitions, it is possible that the western part of the NPO+WPO is originated by the WPO and the eastern part is from the NPO. It is therefore fairly reasonable to assume that the NPO_only indicates pure NPO signature which has been canonically known but the NPO+WPO emanates a combined signature of the NPO and WPO atmospheric patterns to some extent.

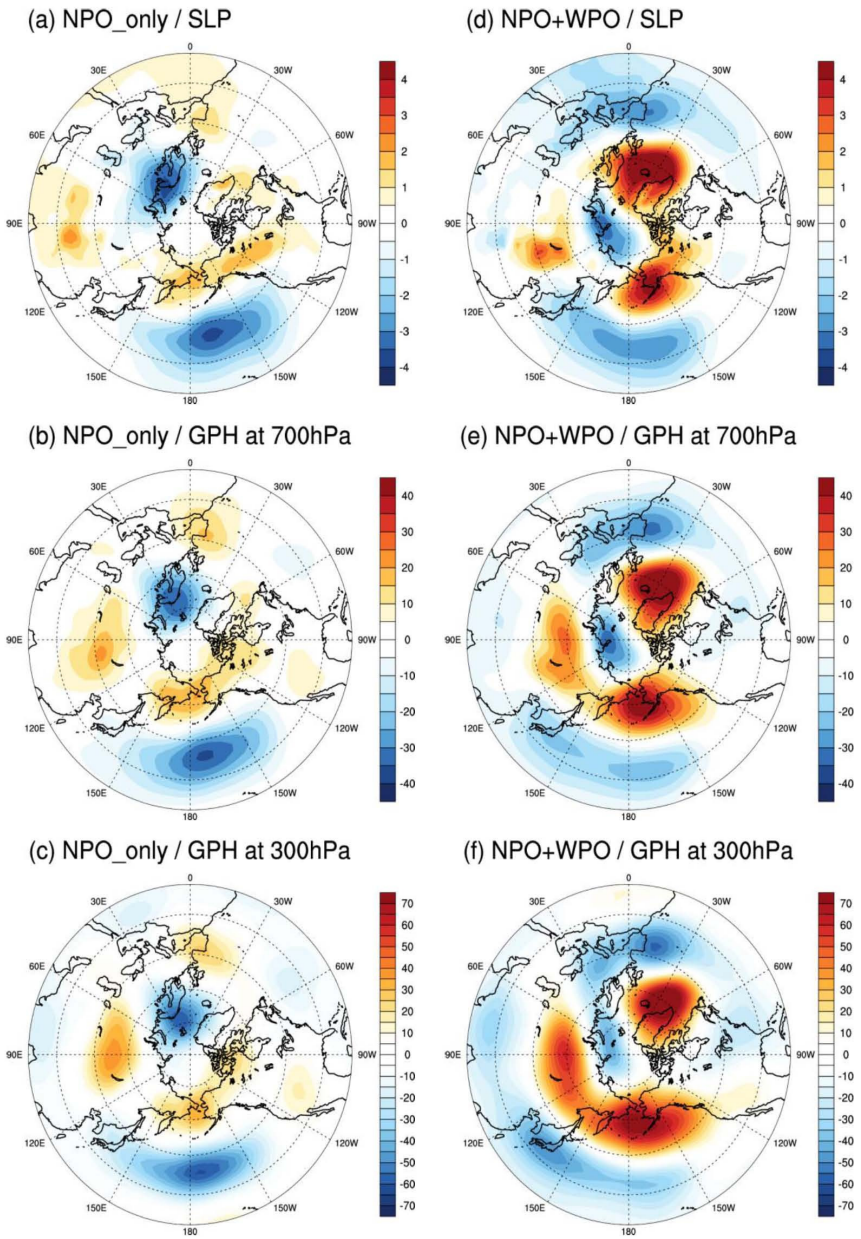

Figure 3 Composites of the anomalous (a) sea level pressure (SLP, in hPa), (b) geopotential height (GPH, in m) at 700 hPa, and (c) 300 hPa during boreal winter (NDJFM) for the NPO_only case. (d), (e), and (f) are the same as (a), (b), and (c), except that they represent the NPO+WPO case. Shading intervals are 0.5 hPa for SLP and 5 m for GPH, respectively.

In order to examine the differences between NPO and WPO in more details, the vertical structures of the GPH and air temperature anomalies at two fixed longitudes for the NPO_only and NPO+WPO are illustrated in Fig. 4. Latitude-height cross sections between 20° and 90°N at 1,000 and 100 hPa along the longitudes of 170°W and 135°E (i.e., the longitudes of maximum geopotential amplitude in both cases as shown in Fig. 3) are presented. Along the 170°W, the GPH and temperature perturbations of the NPO_only have some resemblance to those of the NPO+WPO (Fig. 4(a) and 4(c)), having a north-south dipole GPH pattern with hydrostatically balanced temperature distributions showing that maximum cooling (warming) beneath the upper-level trough (ridge) in the low (high) latitude region. These signs are generally reversed with a nodal line on the maximum GPH anomalies near the tropopause. One may also find that the vertical atmospheric structures of the NPO+WPO are moved equatorward by about 5° when compared to those of the NPO_only. This equatorward moving of the NPO+WPO is presumably due to the expanded strong positive GPH anomalies located in the high latitudes centered at 60°N. As discussed, these positive GPH anomalies are likely to be associated with variability in the Arctic region, such as the strength of the polar jet stream. This issue will be more specifically elaborated in the next section.

Another obvious discrepancy between the NPO_only and the NPO+WPO is found at 135°E (Figs. 4(b) and 4(d)). In the NPO+WPO (Fig. 4(d)), the aforementioned atmospheric features are readily detected, except that the dipole structures are vertically elongated and shifted upwards, which explains why the WPO signature is developed as height increases as shown in Figs. 3(d)–(f). However, there are no notable atmospheric perturbations in the NPO_only at 135°E in spite of weak negative GPH and cold temperature anomalies in lower latitudes (Fig. 4(b)). This is consistent with the previous result that the atmospheric structure of the NPO_only indicates the pure NPO signature.

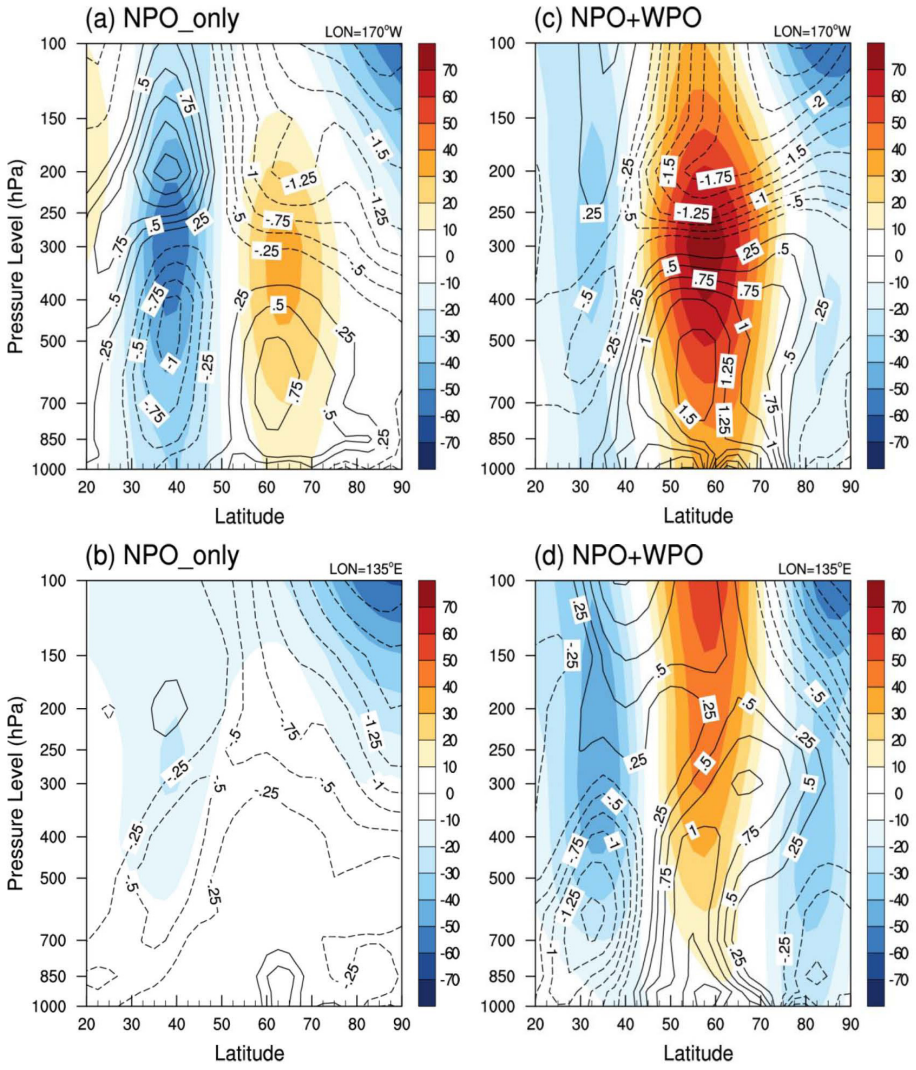

Figure 4 Geopotential height (colored, in m) and air temperature (contour, in °C) anomalies during boreal winter (NDJFM) for the NPO_only case along (a) 170°W and (b) 135°E. (c) and (d) are the same as (a) and (b), except that they represent the NPO+WPO case. Height is colored at 10 m and air temperature at 0.25°C intervals, respectively.

Figure 5(a)-(f) show the conditional composite maps of the detailed SFM process for the NPO_only with relevant atmospheric and oceanic variables. Figure 5(a)-(c) show the anomalous SLP, surface zonal wind and net heat flux during previous winter (ND(-1)JFM(0)). Figure 5(d) and 5(e) show the anomalous SST and zonal wind stress during the following summer (AMJJA(0)) and figure 5(f) shows the SST anomalies during the following winter (OND(0)JF(+1)). As expected, the positive NPO_only forcing transforms surface net heat flux in the North Pacific via changes in the surface wind speed and consequently imparts an SST footprint onto the North Pacific (Figs. 5(a)-(c)). The westerly wind anomalies associated with the southern lobe of the NPO_only forcing exhibit a southward shift in the climatological mid-latitude westerlies so that the strength of trades blown in the central and eastern subtropical Pacific are significantly reduced by the opposite westerly winds and then the large-scale positive net heat flux anomalies (i.e., downward flux into the oceanic surface) are manifested, thereby warming the underlying ocean. This NPO_only-induced SST footprint persists until the following spring and summer (Fig. 5(d)) and the SST anomalies in the subtropical Pacific (0-20oN), in turn, generate zonal wind stress anomalies in the central tropical Pacific (Fig. 5(e)). Although strong westerly wind stress anomalies are observed in the central Pacific, the MM seems to be not well-activated over the North Pacific due to the insignificant warm SST anomalies from the western coast near California to the central tropical Pacific. Nevertheless, canonical El Niño warming signal is clearly observed in the eastern tropical Pacific centered at 110oW during the following winter (Fig. 5(f)). Presumably, that is because the 1997/98 strong El Niño has a very large portion for the whole NPO_only periods (not shown).

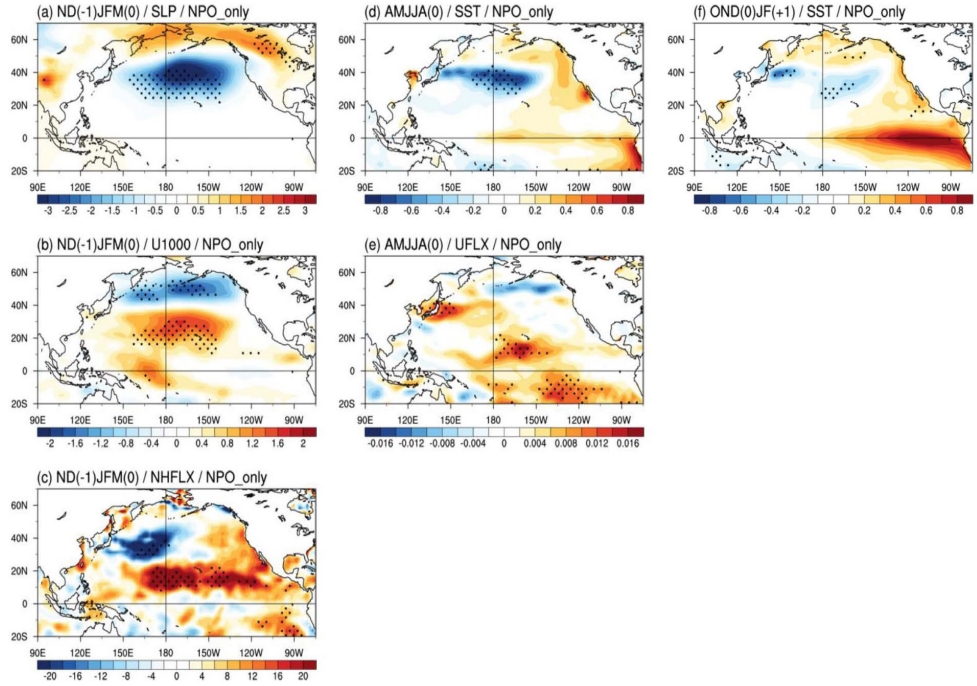

Figure 5 Composites for the NPO_only case of the anomalous (a) sea level pressure (SLP, in hPa), (b) surface zonal wind (U1000, in m/s), (c) surface net heat flux (NHFLX, in W/m^2) during the previous winter (ND(-1)JFM(0)), (d) sea surface temperature (SST, in °C) and (e) zonal momentum flux (UFLX, in N/m^2) during the following summer (AMJJA(0)), (f) SST during the following winter (OND(0)JF(+1)). The surface net heat flux is positive when it has a downward turn. Areas with black dots indicate a 90% confidence level according to a two-tailed Student's *t*-test.

Meanwhile, figure 6(a)-(f) show the same composites as Fig. 5, except for the NPO+WP. The southern lobe of the positive NPO+WP forcing, which contains the WP variability, is more zonally elongated and expanded westward (Fig. 6(a)) when compared to that of the positive NPO_only forcing. Besides, the horseshoe pattern-like positive and negative surface net heat flux anomalies (Fig. 6(c)) make a clear difference from that of the positive NPO_only forcing, which showed a vague dipole structure (see Fig. 5(c)). As inferred by Fig. 6(b), the anomalous negative net heat flux with a nodal line approximately along 40oN is possibly associated with the stronger evaporative cooling due to increasing westerly wind speed in the western Pacific, while the anomalous positive net heat flux in the mid-latitudes (40-60oN) is likely to be related to the pronounced easterly wind anomalies which can reduce the

prevailing westerly winds and subsequently induce less evaporative cooling and northward ocean current anomalies via the theory of the Ekman layer (Holton 2004). These horseshoe-shaped net heat flux anomalies over the North Pacific impart a definite NPGO pattern with strong MM structure in the subtropics during the following summer (Fig. 6(d)). Concurrently, the westerly wind stress anomalies are well-established, mainly located in the north of western equatorial Pacific and easterly wind stress anomalies also exist over the eastern tropical Pacific, broadly centered at 120oW (Fig. 6(e)). According to Kug *et al*. (2009), physical process for an initiation of the central Pacific (CP)-El Niño needs an enhanced easterly wind over the eastern Pacific because it plays a role in suppressing SST warming through upwelling, excess evaporation, and vertical turbulent mixing. Therefore, the CP-El Niño warming is naturally compelled during the following winter (Fig. 6(f)).

As briefly stated, this abnormal warming that has action centers located over the central Pacific or warm pool region, which is distinguished from the traditional canonical feature of ENSO (or the conventional El Niño), there have been many studies to investigate its characteristics. This new type of tropical warming, so far, is referred to as "date line El Niño" (Larkin and Harrison 2005a, b), "El Niño Modoki" (Ashok *et al*. 2007; Weng *et al*. 2007), "warm pool El Niño" (Kug *et al*. 2009). Hereafter, we will use the terminology "central Pacific (CP)-El Niño" for this redefined El Niño and the conventional El Niño type that has its primary SST anomalies centered in the eastern Pacific denote the Eastern Pacific (EP)-El Niño as in Kao and Yu (2009).

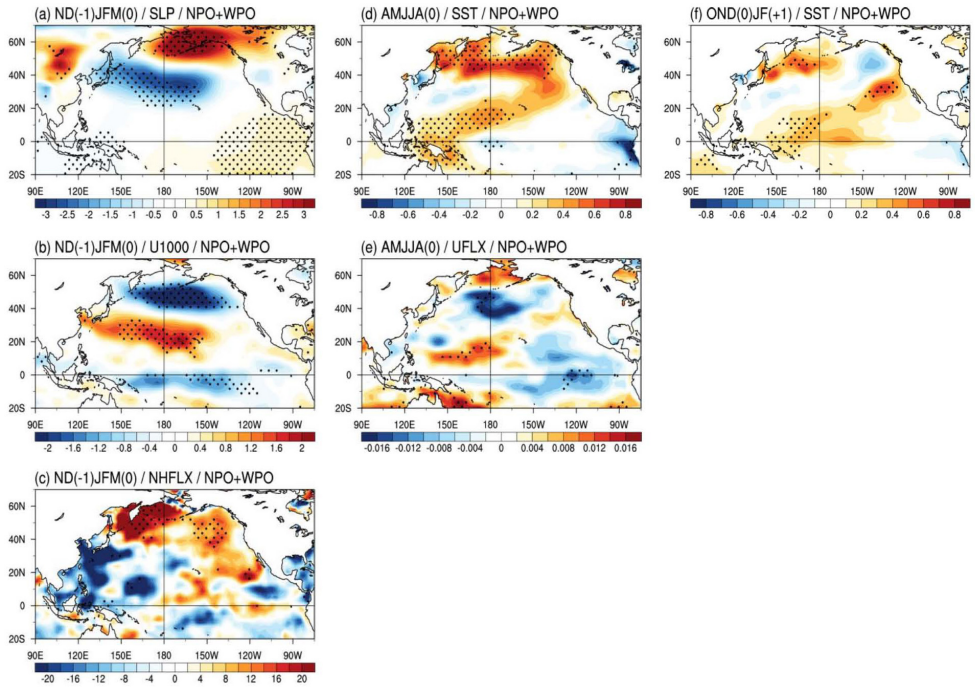

Figure 6 The same as Figure 5, except that they represent th NPO+WPO case.

4.2 Possible interpretations

In this section, we examine the physically plausible interpretations regarding the role of the WPO teleconnection pattern for the SFM process in comparison with the NPO variability. Figure 7 describes the composites of the anomalous SST and horizontal surface winds during the boreal wintertime (NDJFM) for the NPO_only and NPO+WPO cases. Over the North Pacific, it is found that the NPGO-related SST anomaly pattern of NPO+WPO case is significantly clearer than that of NPO_only. In other words, the NPGO-related SST tripole pattern (i.e., a zonal band of negative SST anomalies at around 30oN with positive SST anomalies along 50oN and the positive SST anomaly band that extends toward the central tropical Pacific from the western coast of North America) or SST footprint is well-established when the NPO-like wintertime atmospheric forcing is favorable to the NPO+WPO case. The causal mechanism for this difference has two factors: horizontal wind speeds and

locations. As shown in wind arrows, the anomalous cyclonic circulation for the NPO+WPO is a little bit stronger than for the NPO_only, particularly zonal wind directions around at 30oN (westerly anomalies) and 50oN (easterly anomalies). In addition to this, the westward shift of cyclonic circulation for the NPO+WPO tends to be weakened wind speed anomalies at the eastern edge of the circulation, which induces an anomalous SST warming via the aforementioned WES feedback because the climatological winter mean wind is nearly opposite the anomalous winds. On the other hand, the eastward shift of cyclonic circulation for the NPO_only is more extended to the western boundary of the North American Continent so that the WES feedback is not efficient to impart the SST footprint. Furthermore, it has been reported that the La Niña-like cooling in the equatorial Pacific can contribute to modifying the NPO-like atmospheric forcing and effectively trigger SFM process (Anderson 2007; Alexander *et al.* 2010; Park *et al.* 2012). Hence, the existence of the dominant La Niña-like cooling in the NPO+WPO would be another important factor to generate the strong NPGO pattern but this issue is beyond the scope of this study.

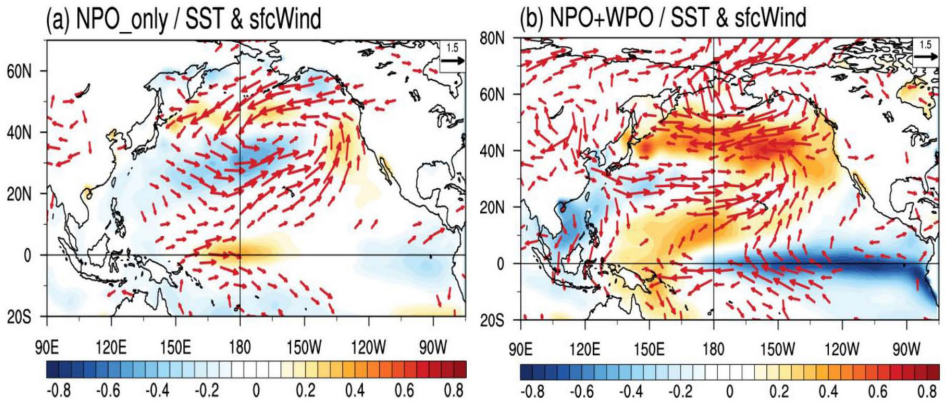

Figure 7 Composites of the anomalous sea surface temperature (colored, in °C) and horizontal surface winds (arrows, in m/s) during boreal winter (NDJFM) for (a) NPO_only case and for (b) NPO+WPO case. The interval in shading for SST is in 0.05°C increments and the wind arrows are only described when their speeds exceed 0.5 m/s. The scale shown by the arrow is expressed in the upper right corner.

Meanwhile, there is another possibility that the WPO pattern has a relation to the variability of the Arctic polar region because the NPO+WPO atmospheric structure shows the enhanced high pressure and positive GPH anomalies over the high latitudes,

roughly including the Arctic region when compared to the NPO_only (see Fig. 3). Also, the dipole pattern of NPO+WPO is significantly moved equatorward by mostly 5 degree as compared to the NPO_only, implying that the polar jet stream is shifted more southward than its climatological location (see Fig. 4). Thus, these two evidences enable us to make a deduction that the WPO variability is intimately associated with the strength of polar vortex during the boreal winter. In order to measure the strength of polar vortex, the intensity of the general zonal circulation in the Northern Hemisphere is investigated using the modified zonal index (ZI_m) suggested by Li and Wang (2003). The ZI_m is defined as the difference in the normalized monthly zonal-mean SLP ($\hat{P}$) between two zones as the annular belts of action in the Northern Hemisphere (i.e., 35oN and 65oN), representing the relative strengths of the subtropical high and sub-polar low. The calculated ZI_m during the boreal winter (NDJFM) periods of 1958-2011 and its correlation map with SLP anomalies are displayed in Fig. 8. As seen, the ZI_m shows an increasing trend until the late 1980s and subsequently shows a decreasing trend (Fig. 8(a)), whose trend changes are fairly analogous to those of the wintertime Arctic Oscillation (AO; Thompson and Wallace 1998) (not shown). The zonally symmetric SLP correlation map with respect to the ZI_m (Fig. 8(b)) is also similar to the typical spatial structure of the AO: positively correlated with the subtropical and mid-latitudes and negatively correlated with the high latitudes and polar region. Therefore, it is quite reasonable to use the ZI_m in order to identify the strength of polar vortex.

Table 2 shows the respective NPO_only and NPO+WPO years and their corresponding ZI_m values. Interestingly, 7 out of 9 years show negative ZI_m values only except for two years (year 1994 and 1996). It is suggested that the positive NPO and WPO forcings are basically linked to a weakened wintertime polar vortex in the Northern Hemisphere. In other words, the NPO and WP variability have a negative relationship (i.e., out-of-phase relationship) with the strength of polar vortex. In particular, the years of the NPO+WPO case have stronger negative ZI_m values (avg. is -2.03) than those of the NPO_only case (avg. is -0.28) so that the strength of polar vortex is largely weakened during the NPO+WPO case, leading to anomalous anti-cyclonic circulations and positive GPH, as shown in Figs. 3(d)-(f). These atmospheric variability are able to expand southward because of the weaker mid-

latitude jet stream, thereby causing the equatorward moving of atmospheric structures, especially larger in the NPO+WPO than the NPO_only.

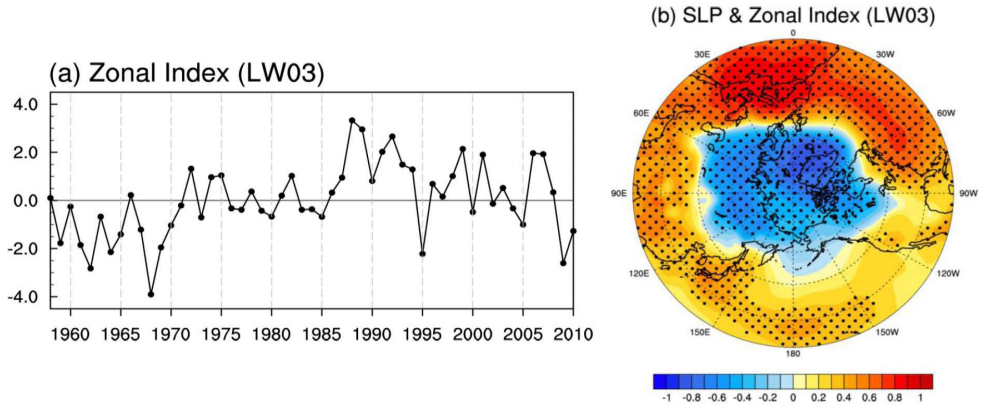

Figure 8 (a) The modified zonal index (ZI_m) during the boreal winter (NDJFM) period of 1958–2011. (b) Correlation map in the Northern Hemisphere between wintertime sea level pressure (SLP, in hPa) anomalies with the ZI_m. The shading interval is in 0.1 increments and areas with black dots indicate a 95% confidence level according to a two-tailed Student's *t*-test.

Table 2 NPO_only and NPO+WPO years and their corresponding modified zonal index (ZI_m) values. Positive (Negative) values are printed in italic (bold) type.

	Year	ZI_m
NPO_only (5)	1964	-2.15
	1977	-0.39
	1980	-0.67
	1994	1.29
	1996	0.52
NPO+WPO (4)	1961	-1.85
	1962	-2.82
	1967	-1.21
	1995	-2.22

4.3 Verification using coupled model

Because the reanalysis data are limited due to the short record in a given period, long-term atmosphere-ocean coupled model data is employed in this study. A 500-yr preindustrial simulation experiment of the GFDL-CM3 CGCM is conducted to verify the observational results (see Sect. 2.2 for more information). Firstly, the tropical SST winter mean climatology and standard deviation of the simulated interannual SST anomaly are computed in Fig. 9. Overall, the spatial structures of the climatological SST and interannual SST variability are comparable to those in observation. The equatorial cold SST bias and the stronger equatorial westward SST gradient in the western and central Pacific, which were manifested in the previous GFDL-CM2.1 model, are substantially attenuated in the present GFDL-CM3 model. Secondly, we examine the first two EOFs (EOF1 and EOF2) of North Pacific SLP anomalies during the winter in order to check the ability for reproducing characteristics of North Pacific wintertime atmospheric variability (not shown). The percent variances explained by EOF1 and EOF2 are 52.1% and 14.0%, respectively, so there is clear separation between EOF1 and EOF2 according to the criterion of North *et al*. (1982). In addition, the spatial structures of the EOF1 and EOF2 clearly show the typical Aleutian Low and NPO-like SLP patterns as the same as observational results.

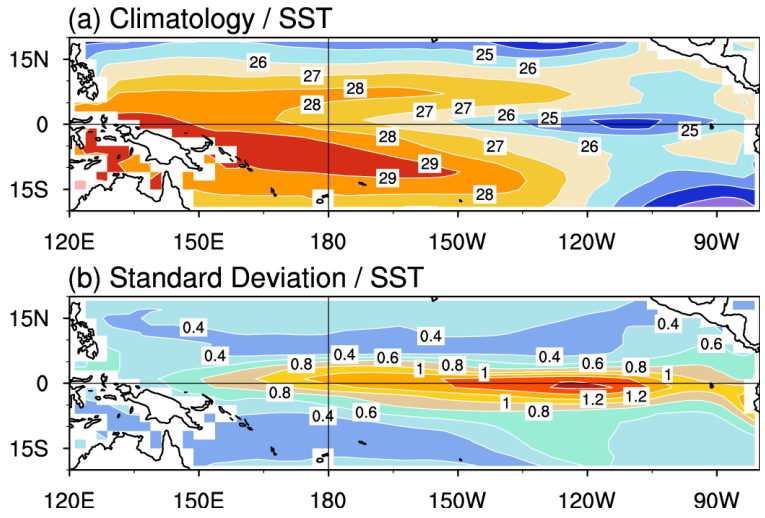

Figure 9 (a) Climatology of sea surface temperature (SST, in °C) over the tropical Pacific during boreal winter (DJF) from the GFDL-CM3 model. (b) Standard deviation of winter SST anomalies. A detailed description of the GFDL-CM3 model is given in Section 2.2.

From the same methodology performed in the observation, conditional composite analysis of SST anomalies for the NPO+WPO and NPO_only cases and their difference during the next winter (D(0)JF(+1)) are displayed in Fig. 10. As in the observation, the El Niño-like SST warming structures are found over the tropical Pacific in both cases, implying that the GFDL-CM3 coupled model is capable of generating the SFM process (Figs. 10(a)-(b)).

However, unlike the observation, both El Niño-like SST warming structures induced by the NPO+WPO and NPO_only prefer to the EP-El Niño pattern with the maximum SST anomaly, which is mainly confined to 120oW. One possibility is that the NPO and WPO indices are not clearly separated due to their strong correlation in the model physics (cf. the temporal correlation coefficient between the NPO and WPO indices is 0.89, which is statistically significant at the 99% confidence level). In spite of the analogous EP-El Niño structures in both cases, significant warm SST anomalies can be discernible in the central-western tropical Pacific including warm pool region, while there are not any prominent changes over the eastern tropical Pacific (Fig. 10(c)). It is suggested that the SFM process induced by the NPO+WP is likely to generate an increasing warming signals over the central Pacific and warm

pool region when compared to the NPO_only, indicating that the NPO+WPO atmospheric forcing highly influences central-western tropical SST variability in the next winter as compared to the NPO_only atmospheric forcing. In conclusion, the model verification using the GFDL-CM3 is not completely consistent with the observational results, but indirectly supports the argument that the wintertime WPO teleconnection pattern has a potential in modulating the ENSO variability during the following winter through the SFM process.

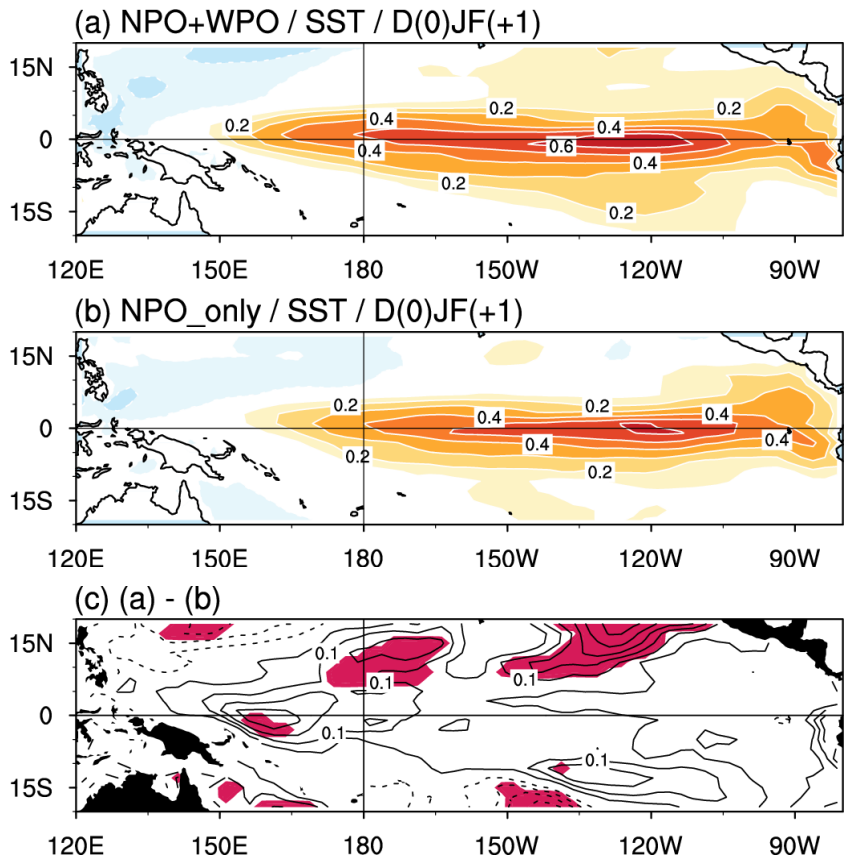

Figure 10 Composite of the anomalous sea surface temperature (SST, in °C) in the GFDL-CM3 model for (a) NPO+WPO case and for (b) NPO_only case during the following winter (D(0)JF(+1)). (c) is the difference between (a) and (b). Solid line (dashed line) denotes positive (negative) values. Contour intervals are 0.1°C in (a) and (b) and 0.05°C in (c), respectively. Shadings in (c) indicate the statistical significant values at 80% confidence level on a Student's *t*-test.

5. Summary and discussion

We explored the role of the WPO teleconnection pattern in changing the SFM process in comparison with the NPO variability using 54 years of observational and 500-yr GFDL-CM3 coupled model simulation data. As a result of the conditional composite analysis, it was realized that the WPO variability could be another feasible

candidate to generate the SFM process, competing with the NPO variability. Furthermore, it was also found that the WPO-induced SFM is associated with the different type of ENSO as compared to the canonical ENSO structure which was generally driven by the NPO-induced SFM process. Therefore, we compared two conditional cases (i.e., NPO_only and NPO+WPO) in order to clarify the specific role of the WP variability and investigate the El Niño spatial structures driven by the SFM processes in each case. Our analysis demonstrated that the NPO_only case indicates pure NPO variability and the NPO+WPO case denotes the WPO-involved NPO variability. In other words, the atmospheric structures of the NPO+WPO forcing were quite different from those of the NPO_only forcing, proving that the NPO and WPO are not the same variability as opposed to the previous arguments that they are dynamically same variability (e.g., Linkin and Nigam 2008). Furthermore, the vertical atmospheric structures of the NPO+WP were shifted equatorward by mostly around 5 degree when compared to those of the NPO_only. This equatorward moving is highly related to the enhanced GPH anomalies and meridional shift of the polar jet stream around the Arctic region. In the NPO+WPO case, the NPO forcing including WPO variability, the NPGO pattern was highly enhanced via activated WES feedback so that warm SST and westerly wind anomalies significantly moved equatorward and finally produced the CP-type El Niño in concurrence with the equatorial easterly wind stress anomalies during the following winter. On the other hand, in the NPO_only case, which is excluding WPO variability, relatively weaker NPGO pattern was derived from inactivated WES feedback, meaning that the SFM process do not play a dominant role although the EP-type El Niño warming appeared in the following winter.

Further analysis suggested the role of the WP teleconnection pattern in changing the SFM process. Firstly, horizontal wind speeds and locations of the NPO+WPO are different from those of the NPO_only. Anomalous cyclonic circulations regarding the positive NPO+WPO forcing are fairly stronger and westward moved than the positive NPO_only forcing so that the WES feedback in the NPO+WPO tends to be more activated and imparts a definite SST footprint over the North Pacific. In addition, the strength of polar vortex has another critical role in controlling the NPO and WPO variability. To calculate the strength of polar vortex, the wintertime modified zonal index (ZI_m), which is introduced in Li and Wang (2003), was adopted and

the corresponding ZI_m values of the respective NPO_only and NPO+WPO years were examined. As a result, both of them were basically associated with a weakening of polar vortex, showing negative AO pattern and particularly the NPO+WPO had stronger negative ZI_m values, leading to intensive anti-cyclonic circulation anomalies over the polar region. These stronger anti-cyclonic circulations in the NPO+WPO are likely to derive the equatorward shift of the mid-latitude atmospheric structure during the winter. Collectively, it is suggested that the WP teleconnection pattern not only has a role in strengthening the SFM process via activating the WES feedback in conjunction with the NPO variability over the North Pacific but also affects the polar vortex strength resulting in the negative AO-like structure. Lastly, using the long-term GFDL-CM3 coupled model pre-industrial 500-yr simulation data, the observational results were indirectly verified because the sample of observation data is limited. Two cases of the NPO+WPO and NPO_only manifested a similar EP-type El Niño warming structure in the following winter, but the NPO+WPO-induced SFM tended to create a center-concentrated SST warming over the tropics than the NPO_only-induced SFM, supporting the observational results.

Consequently, even though the WPO teleconnection pattern has received little research attention due to the similar variability with the NPO, it cannot be ruled out as an important driving factor for the ENSO via the well-established SFM process. This study provided a new perspective of understanding on the connection between the mid-latitude and tropical variability, focusing on the WPO teleconnection pattern.

REFERENCES

Alexander, M. A., 1992: Midlatitude atmosphere-ocean interaction during El Niño. Part II: the Northern Hemisphere atmosphere, *J. Clim.*, 5, 959-972.

Alexander, M. A., I. Blade, M. Newman, J. Lanzante, N. Lau, and J. Scott, 2002: The atmospheric bridge: the influence of ENSO teleconnections on air–sea interaction over the global oceans. *J. Clim.*, 15, 2205–2231.

Alexander, M. A., *et al.*, 2008: Forecasting Pacific SSTs: Linear inverse model predictions of the PDO. *J. Clim.*, 21, 385–402, doi:10.1175/2007JCLI1849.1.

Alexander, M. A., D. J. Vimont, P. Chang, and J. D. Scott, 2010: The Impact of extratropical atmospheric variability on ENSO: Testing the seasonal footprinting mechanism using coupled model experiments. *J. Clim.*, 23, 2885–2901, doi:10.1175/2010JCLI3205.1.

An, S. I., and B. Wang, 2005: The forced and intrinsic low-frequency models in the North Pacific, *J. Climate*. 18, 876-885.

Arkin, P. A., 1982: The relationship between interannual variability in the 200-mb tropical wind field and the Southern Oscillation. *Mon. Wea. Rew.*, 110, 1393-1404.

Ashok, K., S. K. Behera, S. A. Rao, H. Weng, and T. Yamagata, 2007: El Niño Modoki and its possible teleconnection. *J. Geophys. Res.*, 112, C11007, doi:10.1029/2006JC003798.

Barnett, T. P., D. W. Pierce, M. Latif, D. Dommenget, and R. Saravanan, 1999: Interdecadal interactions between the tropics and midlatitudes in the Pacific basin. *Geophys. Res. Lett.*, 26, 615-618.

Barnston, A. G., and R. E. Livezey, 1987: Classification, seasonality and persistence of low-frequency atmospheric circulation patterns. *Mon. Wea. Rev.*, 115, 1083–1126.

Battisti, D. S., 1988: Dynamics and thermodynamics of a warming event in a coupled tropical atmosphere-ocean model. *J. Atmos. Sci.*, 45, 2889–2919

Ceballos, L., E. Di Lorenzo, N. Schneider, and B. Taguchi, 2009: North Pacific Gyre Oscillation synchronizes climate fluctuations in the eastern and western North Pacific. *J. Climate*, 22, 5163–5174.

Chang, P., L. Zhang, R. Saravanan, D. J. Vimont, J. C. H. Chiang, L. Ji, H. Seidel, and M. K. Tippett, 2007: Pacific meridional mode and El Niño–Southern Oscillation. *Geophys. Res. Lett.*, 34, L16608, doi:10.1029/2007GL030302.

Chiang, J. C. H., D. J. Vimont, 2004: Analogous Pacific and Atlantic meridional modes of tropical atmosphere-ocean variability. J. Clim., 17, 4143–4158

Delworth, T. L., and Coauthors, 2006: GFDL's CM2 global coupled climate models. Part I: Formulation and simulation characteristics. *J. Climate*, 19, 634-674.

Di Lorenzo, E., and Coauthors, 2008: North Pacific Gyre Oscillation links ocean climate and ecosystem change. *Geophys. Res. Lett.*, 35, L08607, doi:10.1029/2007GL032838.

Di Lorenzo, E., K. M. C., J. Furtado, N. Schneider, B. Anderson, A. Bracco, M. A. Alexander, and D. Vimont, 2010: Central Pacific El Niño and decadal climate change in the North Pacific. *Nature Geosciences*.

Donner, Leo J., and Coauthors, 2011: The Dynamical Core, Physical Parameterizations, and Basic

Simulation Characteristics of the Atmospheric Component AM3 of the GFDL Global Coupled Model CM3. *J. Climate*, 24, 3484–3519.

Furtado, J., E. Di Lorenzo, B. Anderson, and N. Schneider, 2012: Linkages between the North Pacific Oscillation and central tropical Pacific SSTs at low frequencies. Clim. Dyn., 39, 2833-2846.

GFDL GAMDT, 2004: The new GFDL global atmosphere and land model AM2-LM2:

Evaluation with prescribed SST simulations. *J. Climate*, 17, 4641-4673.

Griffies, Stephen M., and Coauthors, 2011: The GFDL CM3 Coupled Climate Model: Characteristics of the ocean and sea ice simulations. *Journal of Climate*, 24(13), DOI:10.1175/2011JCLI3964.1.

Gu, D., and S. G. H. Philander, 1997: Interdecadal climate fluctuations that depend on exchanges between the tropics and extratropics. *Science*, 275, 805-807.

Hoerling, M. P., A. Kumar, and M. Zhong, 1997: El Niño, La Niña, and the nonlinearity of their teleconnections. *J. Climate*, 10, 1769–1786.

Holton, J. R., 2004: "Chapter 5 – The Planetary Boundary Layer". *Dynamic Meteorology*. International Geophysics Series. 88 (4th ed.). Burlington, MA: Elsevier Academic Press. pp. 129–130.

Hsu, H. H., and J. M. Wallace, 1985: Vertical structure of wintertime teleconnection patterns. *J. Atmos. Sci.*, 42, 1693–1710.

Jin, F. F., 1997: An equatorial ocean recharge paradigm for ENSO.1.Conceptual model. *J. Atmos. Sci.*, 54. 811–829.

Kao, H. Y., and J. Y. Yu, 2009: Contrasting eastern-Pacific and central-Pacific types of ENSO. *J. Climate*, 22, 615–632.

Kistler, R., and Coauthors, 2001: The NCEP-NCAR 50-Year Reanalysis: Monthly Means CD-ROM and Documentation. Bull. Am. Meteorol. Soc., 82(2), 247-268.

Kleeman, R., J. P. McCreary, and B. A. Klinger, 1999: A mechanism for the decadal variation of ENSO. *Geophys. Res. Lett.*, 26, 1743-1747.

Kug J. S, F. F. Jin, and S. I. An, 2009: Two types of El Niño events: cold tongue El Niño and warm pool El Niño. *J. Clim.*, 22, 1499–1515. doi:10.1175/2008JCLI2624.1

Larkin, N. K., and D. E. Harrison, 2005a: On the definition of El Niño and associated seasonal average U.S. weather anomalies. *Geophys. Res. Lett.*, 32, L13705, doi:10.1029/2005GL022738.

Larkin, N. K., and D. E. Harrison, 2005b: Global seasonal temperature and precipitation anomalies during El Niño autumn and winter. *Geophys. Res. Lett.*, 32, L16705, doi:10.1029/2005GL022860.

Lau, N. C., and M. J. Nath, 1996: The role of the "Atmospheric Bridge" in linking Pacific ENSO events to extratropical SST anomalies. J. Clim., 9, 2036-2057.

Linkin, M. E., and S. Nigam, 2008: The North Pacific Oscillation-West Pacific Teleconnection pattern: Mature-Phase Structure and Winter Impacts. J. Clim., 21, 1979–1997.

McPhaden, M. J., and D. Zhang, 2002: Slowdown of the meridional overturning circulation in the upper Pacific Ocean. Nature, 415, 603-608.

Mo, K. C., and R. W. Higgins, 1998: Tropical convection and precipitation regimes in the western United States. *J. Climate*, 11, 2404–2423.

Münnich M, M. Cane, S. Zebiak, 1991: A study of self-excited oscillations of the tropical ocean-atmosphere system. Part II: nonlinear cases. *J. Atmos. Sci.*, 48. 1238–1248

Nakamura, T., Y. Tachibana, M. Honda, and S. Yamane, 2006: Influence of the Northern Hemisphere annualr mode on ENSO by modulating westerly wind bursts. *Geophys. Res. Lett.*, 33, L07709, doi:10.1029/2005/GL025432.

Nakamura, T., Y. Tachibana, and H. Shimoda, 2007: Importance of cold and dry surges in substantiating the NAM and ENSO relationship. *Geophys. Res. Lett.*, 34, L22793, doi:10.1029/2007GL031220.

Newman, M., and P. D. Sardeshmukh, 1998: The impact of the annual cycle on the North Pacific/North American response to remote low-frequency forcing. *J. Atmos. Sci.*, 55, 1336–1353.

Nigam, S., 2003: Teleconnections. Encyclopedia of Atmospheric Sciences, J. R. Holton *et al.*, Eds., Academic Press, 2243–2269.

North, G. R., T. L. Bell, R. F. Cahalan, and F. J. Moeng, 1982: Sampling errors in the estimation of empirical orthogonal functions. *Mon. Wea. Rev.*, 110, 699–706.

Pan, Y. H., and A. H. Oort, 1983: Global climate variations connected with sea surface temperature anomalies in the eastern equatorial Pacific Ocean for the 1958–73 period. *Mon. Wea. Rev.*, 111, 1244-1258.

Park, J. Y., S. W. Yeh, J. S. Kug, and J. Yoon, 2012: Favorable connections between seasonal footprinting mechanism and El Niño. Clim. Dyn., DOI: 10.1007/s00382-012-1477-y.

Rogers, J. C., 1981: The North Pacific Oscillation. *J. Climatol.*, 1, 39–57, doi:10.1002/joc.3370010106.

Straus, D. M., and J. Shukla, 2002: Does ENSO force the PNA? *J. Climate*, 15, 2340–2358.

Suarez, M. J., P. S. Schopf, 1988: A delayed action oscillator for ENSO. *J. Atmos. Sci.*, 45, 3283–3287

Taylor, K. E., R. J. Stouffer, and G. A. Meehl, 2012: An overview of CMIP5 and the experiment design. *Bull. Amer. Meteorol. Soc.*, 485-498.

Thompson, D. W., and J. M. Wallace, 1998: The Arctic Oscillation signature in the wintertime geopotential height and temperature fields. *Geophys. Res. Lett.*, 25, 1297-1300.

Vimont, D. J., D. S. Battisti, and A. C. Hirst, 2001: Footprinting: A seasonal connection between the tropics and mid-latitudes. *Goephys. Res. Lett.*, 28, 3923-3926.

Vimont, D. J., D. S. Battisti, and A. C. Hirst, 2003a: The seasonal footprinting mechanism in the CSIRO general circulation models. *J. Clim.*, 16, 2653–2667.

Vimont, D. J., J. M. Wallace, and D. S. Battisti, 2003b: The seasonal footprinting mechanism in the Pacific: Implications for ENSO. *J. Clim.*, 16, 2668–2675.

Walker, G. T., and E. W. Bliss, 1932: World weather *V. Mem. Roy. Meteor. Soc.*, 4, 53–85.

Wallace, J. M., and D. S. Gutzler, 1981: Teleconnections in the geopotential height fields during the Northern Hemisphere winter. *Mon. Wea. Rev.*, 109, 784–812.

Wang, C. Z., R. H. Weisberg, J. I. Virmani, 1999: Western Pacific interannual variability associated with the El Niño Southern oscillation. *J. Geophys Res.*, 104, 5131–5149.

Weng, H., K. Ashok, S. K. Behera, S. A. Rao, and T. Yamagata, 2007: Impacts of recent El Niño Modoki on dry/wet conditions in the Pacific rim during boreal summer. Climate Dyn., 29, 113–129, doi:10.1007/s00382-007-0234-0.

Wilks, D. S., 2006: Statistical Methods in the Atmospheric Science. Academic Press, San Diego, CA., 648 pp.

Xie, S. P., and S. G. Philander, 1994: A coupled ocean-atmosphere model of relevance to the ITCZ

in the eastern Pacific. Tellus, 46A, 340-350.

Yeh S. W., and B. P. Kirtman, 2008: The Low-Frequency Relationship of the Tropical-North Pacific Sea Surface Temperature Teleconnections. *J. Climate*, 21, 3416-3430.

Yeh S. W., J. S. Kug, B. Dewitte, M. H. Kwon, B. P. Kirtman, and F. F. J, 2009: El Niño in a changing climate. *Nature*, 461, 511–514

Yu, L., and M. M. Rienecker, 1998: Evidence of an extratropical atmospheric influence during the onset of the 1997–98 El Niño. *Geophys. Res. Lett.*, 25, 3537-3540.

Zebiak S, M. Cane, 1987: A model El Niño-southern oscillation. *Mon. Weather Rev.*, 115, 2262–2278

APCC TECHNICAL REPORT 2012-03

- An Assessment of Reliability in Climate Projections : Cloud Variation
- An Evaluation of the Ability of CMIP5 Multi-Models to Predict Interdiurnal Variability
- Climate Change Projection of South Asian Summer Monsoon
- The Role of the Western Pacific Oscillation Teleconnection Pattern

APEC Climate Center

12, Centum 7-ro, Haeundae-gu, Busan 612-020,
Republic of Korea
Tel: +82-51-745-3900 Fax: +82-51-745-3949
www.apcc21.org

비매품
9 788997 133387
ISBN 978-89-97333-38-7
ISBN 978-89-97333-35-6 (세트)